RSC Advances

This is an *Accepted Manuscript*, which has been through the Royal Society of Chemistry peer review process and has been accepted for publication.

Accepted Manuscripts are published online shortly after acceptance, before technical editing, formatting and proof reading. Using this free service, authors can make their results available to the community, in citable form, before we publish the edited article. This *Accepted Manuscript* will be replaced by the edited, formatted and paginated article as soon as this is available.

You can find more information about *Accepted Manuscripts* in the Information for Authors.

Please note that technical editing may introduce minor changes to the text and/or graphics, which may alter content. The journal's standard Terms & Conditions and the Ethical guidelines still apply. In no event shall the Royal Society of Chemistry be held responsible for any errors or omissions in this *Accepted Manuscript* or any consequences arising from the use of any information it contains.

ROYAL SOCIETY OF CHEMISTRY

www.rsc.org/advances

NMR-Based Metabolomics Reveals Distinct Pathways Mediated by Curcumin in Cachexia Mice Bearing CT26 Tumor

Yang Quan-Jun[1,2], Bian Jun[4], Wan Li-Li[1], Han Yong-Long[1], Li Bin[1], Yu Qi[1], Li Yan[1],

Guo Cheng[1,2*], Yang Gen-Jin[3*]

1, Department of Pharmacy, Shanghai Jiao Tong University Affiliated Sixth People's Hospital, Shanghai 200233, P. R. China

2, School of Pharmacy, Shanghai Jiao Tong University, Shanghai 200240, P. R. China

3, School of Pharmacy, Second Military Medical University, Shanghai 200433, P. R. China

4, Department of Pharmacy, No. 411 Hospital of PLA, Shanghai, 200081, P. R. China

*Corresponding author:

Guo Cheng. Shanghai Jiao Tong University Affiliated Sixth People's Hospital, No. 600, Road Yishan, Shanghai, 200233, China. Phone # +86 21 24058098; E-mail: guoc66@gmail.com.

Yang Gen-Jin. School of Pharmacy, Second Military Medical University, Shanghai 200433, P. R. China. E-mail: gjinyang@hotmail.com

RSC Advances Accepted Manuscript

Abstract

Background: Cachexia is common in cancer patients, with profound metabolic abnormalities in response to malignant growth of cancer and progressive catabolism of host. Previous studies showed pharmacodynamics efficacy of curcumin in the prevention and treatment of cancer cachexia. However, the metabolic regulation effect is still unknown.

Methods: We employed proton NMR-metabonomics method to investigate the metabolic features of cancer cachexia and the contribution of curcumin to serum metabolites in a mouse model bearing CT26 tumor.

Results: Curcumin treatment (200 mg/kg/d) resulted in 13.9% less body weight loss and conserved mass of epididymal fat, muscle gastrocnemius and muscle tibialis anterior 91.4%, 11.5%, and 13.7% respectively in cancer cachexia mice. Proton NMR-based metabolomics revealed the altered metabolic profile and found 25 sensitive metabolites associated with cancer cachexia. Moreover, curcumin treatment resulted in metabolic reprogramming including decreasing of phenylalanine, alanine, carnosine, carnitine, taurine, S-sulfocysteine, citrate, malate, glucose, and increasing of citrulline, valine, isoleucine, methionine, glycine, acetoacetate and lactate. The pathway analysis showed the main metabolic regulation of curcumin involved the metabolism of valine, leucine and phenylanaline, and synthesis and degradation of ketone bodies.

Conclusions: These altered metabolic pathways implicate a highly specific metabolism regulation of curcumin and raise the possibility for its therapeutic effect on alleviating cachexia hypermetabolism.

Keywords: Curcumin; Cachexia; Metabolomics; Metabolic pathway; NMR; Branch chain amino acid

RSC Advances Accepted Manuscript

Introduction

Cancer cachexia is a multifactorial syndrome defined by a negative protein and energy balance driven by a variable combination of reduced food intake and abnormal metabolism[1, 2]. This syndrome cannot be fully reversed by conventional nutritional support and leads to progressive wasting of body tissues, in particular loss of muscle mass[3]. The ongoing body and muscle losses are associated with reductions in treatment tolerance, response to therapy, and duration of survival [4]. Previous studies showed that excessive expression of proinflammatory cytokines, such as interleukin 1 β (IL-1β), interleukin 6 (L-6), and tumor necrosis factor-a (TNF-α) are involved in cachexia-related hypercatabolism [5, 6]. These cytokines works through NF-kB, independent pathways such as JAK/STAT, p38, as well as ERK, and act synergistically to activate nuclear transcription factor kappa B (NF-κB) and ubiquitin-mediated proteolytic system, leading to negative energy balance and weight loss [7].

Previous studies suggested that curcumin, as the main active ingredient of turmeric, possess anti-inflammatory activity and exhibited beneficial effects in the treatment of cancer and cachexia[7, 8]. As a natural edible product, it has been traditionally used for the prevention and treatment of metabolic disease over thousands of years [9]. The mechanisms are mainly involved in the inhibition of NF-κB [10, 11], suppression of p38 kinase activity[12], and prevention of cytokine production[10, 13,14]. Inhibition of inflammatory pathways is of particular interest for the energy and protein metabolism[7,15]. *In vitro* study showed that curcumin could modify the metabolism of glutathione, lipid and glucose[16]. Another study confirmed curcumin could attenuate total protein degradation and decrease proteolytic activity of proteasome [7]. An *in vivo* studies also showed that a curcumin complex could prevent weight loss and preserve the weight of the gastrocnemius

RSC Advances Accepted Manuscript

muscle in a murine cachexia model [8]. Moreover, daily intraperitoneal injection of curcumin could inhibit the atrogin-1/MAFbx expression in gastrocnemius and extensor digitorum longus in a dose-dependent manner[17].

Based on the marked metabolic alterations of cancer cachexia and pharmacodynamic effects of curcumin, the global strategy of proton NMR based metabolomics approach is applied to understand the change in metabolites. The aim of the present study is to reveal the metabolic regulation effect of curcumin in a murine model bearing CT26 tumor. We hypothesize that curcumin treatment will lead to the metabolic reprogramming and these may related its mechanisms with reduction of cachexia' catabolic process.

Materials and methods

Animals

All procedures involving animals and their care in this study were approved by the animal care committee of our institution in accordance with institutional requirement and Chinese government guidelines for animal experiments. Five-week-old male BALB/c mice were purchased from Sino-British Sippr/BK Lab Animal Ltd. (Shanghai, China). The mice were kept in conditions of constant temperature and humidity. There were free access to water and identical standard foods for all subjects.

Mouse model bearing CT-26 tumor

The murine CT26 tumor model for inducing cachexia in mice was established as previously described [18-20]. Briefly, fifty-two male BALB/c mice of sixth weeks aged (average body weight 20.61g with SD 1.02 g) were randomly divided into four groups of cachexia (Ca), curcumin-treated cachexia (Cb), curcumin-treated control (Cc), and control (Cd) groups. Cachexia and curcumin-treated cachexia mice were subcutaneously injected with 200ml of CT26

RSC Advances Accepted Manuscript

cell suspension (about 2×10^6 cells in PBS buffer solution) in the left flanks. The other mice were treated equivalently with PBS buffer solution. From the ninth day curcumin-treated cachexia and curcumin-treated control mice were given intraperitoneal injection daily with 200 mg/kg/day curcumin, while the other were treated with 200 ml PBS buffer solution. Curcumin (HPLC purity >98%) was purchased from Feiyu Biological technology co., Ltd (Nantong, China) and the dosage was ascertained by preliminary experiment according with previous study [8,21] . The body weights of the mice were measured every day, and tumor length and width were measured using a digital caliper once the tumor was palpable. The daily food intake was measured and recorded. *In vivo* estimation of tumor weight was calculated using the equation 0.52×length × (width) ^2, which was established by comparing the actual mass with the estimated tumor weight at the end of the experiment as previous study[19]. The body weight was acquired as the whole weight minus the tumor weight. 16 days after tumor inoculation, all mice were euthanized by inhalation of the carbon dioxide. Blood samples were collected into tubes. Heart, epididymal fat, gastrocnemius and tibialis anterior muscles were dissected and weighed. The carcass body was weighted after the tumor was removed.

Proton NMR Spectroscopy of Serum

The serum samples for NMR analysis were prepared by mixing 200 μL of serum with 400 μL PBS buffer solution with pH 7.4 (containing 10% v/v D_2O). All spectra were recorded using Bruker AVANCE II 600 NMR spectrometer operated at 600.13 MHz proton resonance frequency. To attenuate the broad NMR signals from slowly tumbling molecules (such as proteins), standard Carr-Purcell-Meiboom-Gill (CPMG) pulse sequence were used to record the 1D spin-echo spectra. Solvent pre-saturation was also employed to suppress the water peak. Briefly, CPMG pre-saturation pulse sequence worked in the form of −RD-90°-(t-180°-t)$_n$-ACQ, where RD is the

RSC Advances Accepted Manuscript

relaxation delay of 2 s, 90 and 180° represent RF pulses that trip the magnetisation vector, *t* is the spin-echo delay of 400 μs, *n* represents the number of loops (that was 80 in our experiment), and ACQ is the data acquisition period of 1.36 s[22]. In our experiment, the data points were acquired with 128 transients and the number of time domain points was 32k. NMR spectrum was imported into Chenomx NMR Suite 7.7 software (Chenomx, Inc., Alberta Canada) after the pH was calibrated. The metabolites was identified base on the chemical shift, spin-spin splitting and related signal intensity, as described in previous article [23]. Signal assignments were carried out using 2D J-Resolved (jresgpprqf) spectrum. The J-resolved pulse sequence was set up in the form −RD-90°t_1-180°-t_1-ACQ, where t_1 is an incremented time period and the number of scans per increment was 16. After fourier transformation, phase correction and baseline correction were carefully performed using TopSpin 3.0 software package (Bruker Biospin, Rheinstetten, Germany). The proton chemical shifts were referred to methyl doublet signal of lactate (δ1.33). The spectra were then imported to AMIX (Bruker Biospin, Rheinstetten, Germany) and all the spectra were reduced to fixed integral regions (0.05 ppm). The chemical shift range was δ 0.2–8.0 and the regions of δ 4.7-5.1 that contained the resonance from residual water were removed from the dataset. To filter concentration differences between samples, the intensity values corresponding to each NMR spectrum were normalized to the sum of integration value (100%).

Multivariate statistical analysis

Multivariate statistical analysis and pathway analysis of the exported dataset was analyzed using the online software of Metaboanalysis 2.0 (Available: http://www.metaboanalyst.ca/). It is a free, user-friendly, and easily accessible tool for biomarker discovery, classification and pathway mapping. The dataset was arranged with the samples as observations and peak area of chemical

RSC Advances Accepted Manuscript

shift as the response variables. Before the multivariate statistics, response variables was centered and scaled to Pareto Variance with the purpose to enlarge or shrink variables and explorer the subtle distinctions. To make skewed distributions more symmetric, the log transformation were used for the nonlinear conversions of the data.

To interpret the relationship resulting from the treatment of curcumin, principle component analysis (PCA) and Partial Least Squares - Discriminate Analysis (PLS-DA) were employed to extract information from multicomponent measurements and to remove redundant data. The main purpose of PCA is to eliminate the collinear variables and then reduce the dimensionality of the original space. It is an unsupervised method used to reveal the internal structure of dataset in an unbiased way. PLS is a supervised regression method to maximize the covariance between the predictor space and the response space. It can predict responses in the population using the predictor matrix. Three parameters, R^2X, R^2Y and Q^2Y, were used for evaluation of the models. R^2X explains the cumulative variation in the response variables, and R^2Y is the latent variables of the sums of squares of all Xs and Ys. Q^2 reflects the cumulative cross-validated percentage of the total variation that can be predicted by the current latent variables [16, 24]. High coefficient values of R^2Y and Q^2 represent good discrimination and the predictive ability [25,26]. The specific metabolites between classes were interpreted through variable importance in the projection (VIP). Those variables with VIP > 1 were used as responsible metabolites and applied for metabolic pathway analysis.

For the annotating significant features, pathway enrichment analysis and pathway topology analysis of Metaboanalysis was used to identify the most relevant metabolic pathways[27]. Pathway enrichment analysis used GlobalTest and GlobalAncova to analysis the concentration values. Compared with compound lists method, it is more sensitive to identify subtle changes

RSC Advances Accepted Manuscript

involved in the same biological pathway. To focus on global network topology analysis, relative betweenness centrality was used for metabolite importance measure. This allowed ordering the metabolic pathway by their positions. The changes in a more important node of the network would trigger a more severe impact on the pathway than changes occur in marginal or relatively isolated positions.

Statistics

Data of body characteristics and biochemical parameters were presented as means±SD. Results was compared with one-way ANOVA followed by Tuckey's test with the software IBM SPSS 20.0. The value of p less than 0.05 in two-tailed tests was regarded as statistically significant.

Results

Curcumin preserved the body weight of cancer cachexia mice

Inoculation of CT26 adenocarcinoma cells into BALB/c mice resulted in typical cachexia syndrome with a progressive loss of body weight. The body weight declined 28.52% after16 days, from control of 15.95±0.98 g to the cachexia state of 11.40±0.89 g (Table 1). The mass of epididymal fat, muscle gastrocnemius and tibialis anterior were decrease 79.10%, 34.71%, and 7.85% respectively. Moreover, the organ weight of heart, lung and kidney were significant decreasing. The spleen weight was increased from normal 128.33±9.73 mg to 225.45±53.79 mg, prompting an excessive elaboration of immune response. The 16 days accumulated food intake of cancer cachexia was only decreased 2.08% compared with control group, which was agreed with previous study that cancer cachexia has no remarkable influence on food intake [19]. These

RSC Advances Accepted Manuscript

results indicated the loss of body weight and atrophy of skeletal muscle in cachexia animal was mainly caused by the progressive of metabolic disruption, rather the the loss of appetite and reduction of food intake.

200 mg/kg/d curcumin treatment resulted in the alleviate of tumor burden by reducing the tumor weight from 3.03 ± 0.55 to 2.36 ± 0.80 g, as well as preserve 13.88% body weight. Moreover, compared with the cancer cachexia mice, the weights of epididymal fat, muscle gastrocnemius and tibialis anterior form curcumin-treated cachexia mice increase 91.44%, 11.51%, and 13.73% respectively. However, treatment with curcumin on control mice resulted in significantly increase of spleen and liver weight, as well as decrease of epididymal fat. The increased liver weight may indicate some hepatotoxicity of curcumin. So the serum alkaline phosphatase (ALP), glutamic - pyruvic transaminase (GPT) and glutamic - oxaloacetic transaminase (GOT) were measured. Compared with control mice with 200 mg/kg/d curcumin-treated control mice, there was no significant difference of ALP and GPT, the single high of GOT may mean acute liver injury or muscle metabolism. These implied the negligible hepatotoxicity of curcumin.

Metabolites analysis of cancer cachexia mice and effect of curcumin

The blood biochemical responses were listed in table 2. Hypoglycemia and disorders of hepatic functions could be found from the blood biochemical examination during the time of the weight loss in cancer cachexia mice[18].Tumor-induced cachexia resulted in the falling of glucose concentration from normal 7.34 to 2.72 mM/L. The glycated albumin was also decreased from 9.87% to 6.17%. Moreover, the VLDL level of cachexia group was 9 fold higher than control group, while the HDL was forty percents of control group. Triglyceride was also elevated from 1.24 to 3.56 mM/L, almost 3 folds of control group. What is more, the free fatty acids of blood

RSC Advances Accepted Manuscript

variation were also decreasing 29.76%, from 1428.00 to 1003.67μEq/L. These data imply disturbance of lipid and glucose metabolism. The impairment of muscle metabolism was also suggested by the significantly elevated level of CK-MB (34.15%) in the cachexia mice.

Based on these alternations of metabolic imbalance, a systemic metabolomics approach was established to reveal the metabolic profile and role of curcumin as an antagonist of cachexia. In our study, proton NMR spectra were employed for its capability of detecting all organic compounds with high reproducibility and robust statistics. The typical serum NMR spectra from the four groups were obviously different (Figure 1). The identification of metabolites was done by comparing the signals with the reference NMR spectra in the Chenomx and HMDB database. The high-intensity signal at δ1.18 with a wide protein peak in the spectrum was lipid CH_2 of lipoprotein (VLDL and LDL), as described in previous study [28]. However, the 1D spectrum could not discriminate the overlapping signals, such as isopropyl of leucine and valine. So 2D J-resolved spectrum experiment was employed to show the spin-spin splitting information on the second axis. With the help of 2D J-resolved spectrum for detecting the splitting patterns and coupling constants, not only the isopropyls from leucine and valine were assigned, but also the metabolites which were overlapped with the congested regions of the sugar region (δ 3.2–3.8) were identified (Figure 2).

Global metabolic profile of cancer cachexia and curcumin

In order to reveal global metabolic profile, PCA was firstly applied to display the groups and trends of the samples. The score plot of the first two score vectors revealed that the cancer cachexia and control mice were obviously different. To relate the metabolites to the groups and discriminate the class belongings, PLS-DA approach was then employed (Figure 3). The model was statistical validated with R^2X (cum) 0.419, R^2Y (cum) 0.812, and Q^2 (cum) 0.659,

RSC Advances Accepted Manuscript

respectively. Curcumin treatment resulted in the significant different trends, suggesting that curcumin treatment could reduce the effect of the tumor on metabolic profile. In addition, cancer cachexia trigger the changes of metabolites, such as lactate (δ 1.33, δ 4.15), alanine (δ 1.48), creatine (δ3.04), taurine (δ 3.25, δ 3.42), glycine (δ 3.59), and glucose (δ 4.66 and 5.23). The relative levels of partial metabolites were listed in Figure 4.

Cancer cachexia related metabolic disorder

Though the corresponding loading plot could indicate the peak assignment associated with the four groups, it is difficult to screen the unique metabolites associated with cancer cachexia. In order to identify the altered metabolites of cancer cachexia, a separated PLS-DA model was employed to distinguished cancer cachexia from healthy control mice. Cachexia group was remarkable distributed out of the region of control group. The signal with VIP >1 was assigned and the intensity value with significant different was analyzed. A total of 25 changed metabolites were identified related with cancer cachexia, including decreased levels of citrulline (δ 6.36, δ 3.74), carnitine (δ3.17), taurine (δ 3.25, δ 3.42), S-sulfocysteine (δ 3.66, δ 3.48), citrate (δ2.55, δ2.69), glycine (δ 3.59), leucine (δ 0.96), valine(δ 1.06), isoleucine (δ3.67, δ1.02), glucose (δ 4.66 δ 5.23), and increased phenylalanine (δ7.39, δ4.00), alanine (δ 1.47), methionine (δ2.14), carnosine (δ2.66, δ3.22, δ7.08), lactate (δ 1.33, δ 4.15), VLDL/LDL (δ 1.19), choline (δ3.22), acetoacetate (δ 2.28), trans-aconitate (δ3.45), pyruvate (δ 2.32), asparagine (δ 3.97, δ 2.81), creatine (δ3.04), 3-hydroxybutyrate (δ 2.28, δ 1.19), glutamine (δ 2.33) and UDP-glucose (δ4.27, 4.36). The metabolic disorders were associated with aerobic glycosis, with the result of attenuation of glucose entry into the Krebs cycle. Through the induction of lactate dehydrogenase and pyruvate dehydrogenase, the diversion of pyruvate to lactate resulted in decreasing flux from pyruvate to acetyl-CoA. These alterations were agreed with previous

RSC Advances Accepted Manuscript

reported "Warburg effect". To search the unique metabolites of cachexia, we compared the cancer mice (tumor-bearing mice without body weight loss) with cachexia mice (tumor-bearing mice with significant body weight loss) of previous results [19]. From the score plot, we also found that cachexia animals separated dramatically from cancer. These altered metabolites prompt the cachexia-related hypercatabolism came in the glycolysis, lipolysis, citrate cycle and amino acid metabolic alteration. It is notable that the diversion of pyruvate to lactate led to the depletion of glycine and alanine. To meet the need of energy, excess glucose and fatty acids was consumed, associated with the accumulated intermediate metabolites, and thus resulted in hypoglycemia as well as insulin resistance, severe inflammation and negative energy balance [29, 30].

Curcumin regulated the metabolic pathway of health control and cancer cachexia mice

Based on the effect of curcumin on regulation of metabolism, the PLS-DA model containing the dataset of curcumin and cachexia groups was established as previous described. Scores plot (Figure 5A) showed the obvious separations of the two groups along PC1 (47.5% of the variance), and PC2 (11.7% of the variance) with satisfactory predictive abilities ($R^2Y(cum)$ =0.868, and Q^2 (cum) = 0.906). Loading plot analysis illustrated the major metabolites which was resulted of curcumin treatment including increasing of leucine, isoleucine, valine, citrulline, taurine, s-sulfocysteine, citrate, malate, acetoacetate, glucose, and decreasing of pyruvate, phenylalanine, 3-hydroxybutyrate, VLDL/LDL, choline, methionine, 2-oxovalerate, carnosine, glycine, carnitine, lactate, trans-aconitate, lactate and UDP-glucose. These data revealed that curcumin treatment could regulate the metabolic profile of cancer cachexia mice including reprogramming the glycolysis and adjust the citrate cycle and amino acid metabolism.

To further investigate the serum distinct endogenous metabolites resulting from curcumin treatment, a visual profile of PLS-DA model was assessed to show the separate treatment group

RSC Advances Accepted Manuscript

from health control mice (Figure 5B). The score plot indicated significant discrimination with satisfactory predictive abilities (R2Y (cum) =0.962, and Q2 (cum) = 0.993). Curcumin treatment resulted in regulation of metabolic profile including decreasing of phenylalanine, alanine, carnosine, carnitine, taurine, S-sulfocysteine, citrate, malate, glucose, and increasing of citrulline, valine, isoleucine, methionine, glycine, acetoacetate and lactate. These metabolites implied the regulation of curcumin on taurine, fatty acid and ketones metabolism.

Detailed analysis of pathways and networks influenced by curcumin were performed with MetPA. Result of the pathway analysis was shown in Figure 6. Here the biological pathway analysis revealed that the changed metabolites were mainly involved in the valine, leucine and isoleucine biosynthesis, synthesis and degradation of ketone bodies, taurine and hypotaurine metabolism, glycerolipid metabolism, and glycine, serine and threonine metabolism (Table 3). Valine, leucine and isoleucine biosynthesis was the most impact pathways, which was calculated from pathway topology analysis. Three matched metabolites of valine, leucine, and isoleucine were gradually reduced and the statistical difference was significant from the p value.

Discussion

This study reveals the specific metabolic profile of cancer cachexia and the contribution of curcumin for the metabolic reprogramming in the murine cachexia model bearing the CT26 tumor. The BALB/c mice showed typical cachexia characteristic with a decrease in body weight and lean mass. Curcumin treatment prevented the body and muscle weight loss as well as regulated the metabolic profiles of model mice, including increase of branch chain amino acids (BCAA), decrease of phenylanaline, and changed ratio of 3-hydroxybutyrate to acetoacetate. BCAA includes valine, leucine and isoleucine. They were not only important regulator in muscle protein turnover, but also promote protein synthesis and increase muscle mass[31, 32]. BCAA are

RSC Advances Accepted Manuscript

the only amino acids that mainly metabolized in skeletal muscle. In the case of the shortage of energy in muscle, BCAA are catabolized for synthesis of acetyl-CoA, and thus are termed as glucogenic amino acids. When BCAA supplies become restricted, mammalian cells, in particular muscle cells, employ homeostatic mechanisms to rapidly inhibit protein synthesis and subject to high protein turnover[32]. Mammalian target of rapamycin (mTOR) is a key mediator of protein translation and gene transcription. Studies showed leucine can interact with mTOR pathway and increase the protein synthesis rate and protein translation[33]. The decreases of serum BCAA would result in the underactive of mTOR and imply the negative nitrogen balance of muscle[34].

Phenylalanine is an aromatic amino acid (AAA) and mainly metabolized in the liver. The ratio of BCAA and AAA reflects the homeostasis disorder, and may obstruct the physiologic function. However, curcumin treatment resulted in the amelioration of amino acid metabolism. The abnormally elevated phenylalanine was decreased and the attenuated levels of BCAA were increased. The mobilizations of essential amino acids were consistent with hypermetabolism of glutamine, asparagines, alanine and creatine, derived by glutamic-pyruvic transaminase. These results suggested cachexia was associated with an alternative amino acid metabolic feature and contribution of curcumin to the cachexia syndrome partly resulted from the redress of the metabolic imbalance.

The progressive deterioration in nutrition status was primarily arisen from the utilization of glucose by the tumor. Malignant growth of cancer leaded to the aerobic glycolysis, resulting in the attenuation of Krebs Circle. To maintain relatively metabolic homeostasis, hypoxia inducible factor mediated the diversion of engrgy metabolism from pyruvate to lactate, rather than the flux from pyruvate to aceryl-CoA [35]. The hypermetabolism of glycolysis also cause the lipid

RSC Advances Accepted Manuscript

mobilization and hypoglycemia [36]. However, clinical and fundamental researches suggest that conventional nutritional support has little effect on reversing the body and lean weight. So we analysis the metabolic profile of cancer cachexia and the contribution of curcumin on the imbalance metabolism. NMR spectrum provided evidences of enhancing lipolysis without elevated concentration of ketone bodies after curcumin treatment. As previous results of lipid metabolism resulted from cancer[28], we found detailed perturbations of endogenous small molecule intermediate included high levels of lactate, glycerol, acetone, acetoacetate, and 3-hydroxybutyrate. During the cachexia period, the ketone body ratio of 3-hydroxybutyrate to acetoacetate was increase from normal 1:1 to as high as 5:1.High levels of ketones refer to the deleterious effect [37]. After curcumin treatment, the ketone ratio was restored to 2:1 by the significant decreasing of 3-hydroxybutyrate[38].

The metabolic reprogramming of cancer cachexia was independent with nutritional deficit, as the accumulated food intake was not significant different among the groups of cachexia and control. However, the implantation of tumor caused markedly splenomegaly and immunological reaction, resulting in the releases of proinflammatory cytokines, such as TNF-α, IL-6, IL-1β and INF-γ. These cytokines are associated with activation nuclear transcription factor kappa B (NF-κB) and downstream ubiquitin-mediated proteolytic system, which was responsible for the degradation of muscle protein and weight loss [39]. Curcumin, as an anti-inflammatory ingredient of turmeric, possess the potential of adjusting the metabolic profile and redress the metabolic imbalance.

In conclusion, high resolution proton NMR based metabolomics revealed 25 changed metabolites of cancer cachexia and the metabolic regulation effect of curcumin in the murine model bearing CT26 tumor. Based on the changed serum metabolite, curcumin treatment

RSC Advances Accepted Manuscript

resulted in the redress of metabolic imbalance, including the increase of BCAA, decrease of phenylanaline, and the changed ratio of 3-hydroxybutyrate to acetoacetate. These results indicate the mechanism of curcumin for the preserve of body and muscle weight was due to the reduction of cachectic catabolic process. The distinct pathways of curcumin on BCAA and ketone body metabolism imply the potential for its usage in the prevention and treatment of cancer cachexia.

Competing financial interests

The authors declare no competing financial interests.

Acknowledgements

The authors thank Fu Yao for the help of animal care. This investigation received financial support from the National Basic Research Program (No. 81072687), Shanghai Pharmaceutical Association (No. 2014-YY-01-08) and College Subject of Shanghai Jiao Tong University affiliated Sixth People's Hosptial (No. ynlc201420).

RSC Advances Accepted Manuscript

Table1 Effects of curcumin on body characteristics

	Ca (13)	Cb (12)	Cc (13)	Cd (13)
Tumor(g)	3.03±0.55	2.36±0.80$^{\#}$		
Carcass weight(g)	11.4±0.89*	12.98±1.09$^{*\#}$	15.08±1.61	15.95±0.98
Heart(mg)	107.91±18.51*	111.40±14.23*	143.08±22.46	159.17±32.01
Lung(mg)	136.27±13.46*	161.40±14.68$^{*\#}$	177.67±21.58	172．00±29.18
Liver(mg)	937.01±85.10*	1170.50±157.29$^{\#}$	1251.50±163.25*	1145.00±88.64
Spleen(mg)	225.45±53.79*	331.20±88.25$^{*\#}$	268.5±63.75*	128.33±9.73
Kidney(mg)	283.18±105.62*	336.29±36.64$^{*\#}$	400.83±39.52	392.42±45.74
Gastrocnemius muscle(mg)	187.10±43.03*	208.64±73.51$^{*\#}$	275.42±23.70	286.58±16.55
Tibialis anterior muscle(mg)	103.10±41.37*	120.02±59.59$^{\#}$	129.58±15.11	133.58±24.91
Epididymal fat (mg)	81.54±61.37*	128.50±30.42$^{*\#}$	246.00±106.64*	389.92±96.94
Food intake (g)	619.2	616.8	612.7	632.4

Data were shown as mean ± SD. * represented significantly difference between Ca, Cb and Cc with Cd ($p < 0.05$). $^{\#}$ represented significantly difference between Cb with Ca($p < 0.05$). Ca: Cachexia; Cb: Curcumin treatment of Cachexia; Cc: Curcumin treatment of control; Cd: Control.

Table 2 Effects of curcumin on biochemical parameters

	Ca (13)	Cb (12)	Cc (13)	Cd (13)
Triglyceride(mM/L)	3.56±1.78*	3.85±0.87*	1.87±0.65*	1.24±0.37
HDL(mM/L)	0.88±0.17*	1.87±0.79$^{*\#}$	2.20±0.17	2.13±0.12
VLDL(mM/L)	0.65±0.15*	0.46±0.15$^{*\#}$	0.07±0.06	0.07±0.04
Creatine(μM/L)	6.50±2.07*	9.86±3.49$^{\#}$	10.27±3.74	9.27±4.06
Glucose(mM/L)	2.72±0.87*	6.93±0.88$^{\#}$	6.75±0.90	7.34±1.34
Glycated albumin(%)	6.17±3.76*	7.46±2.52$^{*\#}$	9.96±3.72	9.87±3.60
ALP	221.47±18.86*	244.25±36.24$^{*\#}$	42.15±18.24*	35.83±10.38
GPT	59.50±7.06*	68.65±48.25$^{*\#}$	37.96±18.51	43.73±5.62
GOT	930.67±147.53*	623.51±252.62$^{*\#}$	188.42±34.05	110.27±14.03
Creatine kinase(U/L)	941.50±183.96*	1186.21±204.00$^{*\#}$	1046±341.23	1058.91±298.11
CK-MB(U/L)	741.50±126.30*	642.34±98.40$^{*\#}$	522.70±167.55	552.73±147.66
Urea(mM/L)	11.05±2.62*	6.92±2.42$^{\#}$	8.40±0.67*	7.60±0.82
FFA(μEq/L)	1003.67±299.21*	1136.26±261.36$^{*\#}$	1351.28±325.49	1428.00±291.12

Data were shown as mean ± SD. * represented significantly difference between Ca, Cb and Cc with Cd ($p < 0.05$). $^{\#}$ represented significantly difference between Cb with Ca($p < 0.05$). Ca: Cachexia; Cb: Curcumin treatment of Cachexia; Cc: Curcumin treatment of control; Cd: Control. HDL: High density lipoprotein; VLDL: Very low density lipoprotein; ALP: Alkaline phosphatase; GPT: Glutamic-pyruvic transaminase; GOT: Glutamic-oxalacetic transaminease; FFA: Free fatty acids; CK-MB: Creatinine kinase isoenzyme MB

RSC Advances Accepted Manuscript

Table 3 Altered pathway analysis of curcumin with MetPA

	Total Cmpd	Hits	Raw p	-LOG(p)	Holm adjust	FDR	Impact
Valine, leucine and isoleucine biosynthesis	11	4	1.48E-06	13.421	3.86E-05	8.91E-06	0.99999
Synthesis and degradation of ketone bodies	5	2	0.011015	4.5085	0.033045	0.011802	0.60000
Taurine and hypotaurine metabolism	8	1	0.007476	4.8961	0.030689	0.008307	0.42857
Glycerolipid metabolism	18	1	0.000326	8.0277	0.0045684	0.000576	0.28098
Glycine, serine and threonine metabolism	31	5	9.33E-08	16.188	2.70E-06	1.23E-06	0.26884
Glyoxylate and dicarboxylate metabolism	18	1	0.0122	4.4064	0.033045	0.01262	0.25806
Pyruvate metabolism	23	2	8.17E-05	9.4127	0.0013886	0.000163	0.18375
Alanine, aspartate and glutamate metabolism	24	3	3.12E-07	14.981	8.41E-06	2.34E-06	0.14979
Citrate cycle (TCA cycle)	20	2	5.13E-05	9.878	0.0010065	0.000128	0.1254
Cysteine and methionine metabolism	27	2	5.03E-05	9.897	0.0010065	0.000128	0.10977
Butanoate metabolism	22	3	3.51E-05	10.257	0.00073737	0.000105	0.10145
Glycolysis or Gluconeogenesis	26	2	8.17E-05	9.4127	0.0013886	0.000163	0.09891
Primary bile acid biosynthesis	46	2	0.000303	8.1017	0.0045454	0.000568	0.05952
Arginine and proline metabolism	44	3	1.23E-07	15.914	3.43E-06	1.23E-06	0.05612
Starch and sucrose metabolism	19	1	0.002325	6.0642	0.023247	0.003321	0.03958
Galactose metabolism	26	2	1.14E-05	11.378	0.00027476	4.76E-05	0.03644
Glycerophospholipid metabolism	30	1	1.27E-05	11.275	0.0002919	4.76E-05	0.02315
Glutathione metabolism	26	1	0.00341	5.6811	0.030689	0.004092	0.00573

Total Cmpd is the total number of compounds in the pathway; the Hits is the actually matched number from the user uploaded data; the Raw p is the original p value calculated from the enrichment analysis; the Holm p is the p value adjusted by Holm–Bonferroni method; the FDR p is the p value adjusted using False Discovery Rate; the Impact is the pathway impact value calculated from pathway topology analysis.

RSC Advances Accepted Manuscript

Figure legends

Figure 1. Representative 600MHz proton NMR spectrum of serum from cachexia (Ca), curcumin-treated cachexia (Cb) and curcumin-treated control (Cc) and control (Cd) mice. The spectrum displayed a wide range of metabolites such as carbohydrates, lipoproteins, organic acids and amino acids.

Figure 2. The typical 2D J-resolved NMR spectroscopy of serum metabolites.

Figure 3. 2D PLS-DA score plots showed significant discrimination of the cachexia (Ca), curcumin-treated cachexia (Cb) and curcumin-treated control (Cc) and control (Cd) mice.

Figure 4. The relative levels of serum metabolites of cachexia (Ca), curcumin-treated cachexia (Cb), curcumin-treated control (Cc) and control (Cd) groups.

Figure 5. The PLS-DA score plots between two groups: cachexia (Ca) and curcumin-treated cachexia (Cb) revealed the curcumin effect on cancer cachexia mice (A), and curcumin-treated control (Cc) and control (Cd) identified regulation of curcumin on control mice.

Figure 6. The perturbed metabolic pathways of cachexia and the effect of curcumin. The X axis was the impact factor and the Y axis was the –log(p).

RSC Advances Accepted Manuscript

References

1. K. Fearon, J. Arends and V. Baracos, *Nature reviews. Clinical oncology*, 2013, **10**, 90-99.
2. K. Fearon, F. Strasser, S. D. Anker, I. Bosaeus, E. Bruera, R. L. Fainsinger, A. Jatoi, C. Loprinzi, N. MacDonald and G. Mantovani, *The lancet oncology*, 2011, **12**, 489-495.
3. N. Jacquelin-Ravel and C. Pichard, *Critical reviews in oncology/hematology*, 2012, **84**, 37-46.
4. C. L. Donohoe, A. M. Ryan and J. V. Reynolds, *Gastroenterology research and practice*, 2011, **2011**, 601434.
5. M. J. Delano and L. L. Moldawer, *Nutrition in clinical practice : official publication of the American Society for Parenteral and Enteral Nutrition*, 2006, **21**, 68-81.
6. Y. Fong, L. L. Moldawere, W. He, M. Marano, C. V. Keogh, J. Gershenwald and S. F. Lowry, *Surgical oncology*, 1992, **1**, 65-71.
7. S. M. Wyke, S. T. Russell and M. J. Tisdale, *British journal of cancer*, 2004, **91**, 1742-1750.
8. R. A. Siddiqui, S. Hassan, K. A. Harvey, T. Rasool, T. Das, P. Mukerji and S. DeMichele, *The British journal of nutrition*, 2009, **102**, 967-975.
9. M. Salem, S. Rohani and E. R. Gillies, *RSC advances*, 2014, **4**, 10815-10829.
10. C. Jobin, C. A. Bradham, M. P. Russo, B. Juma, A. S. Narula, D. A. Brenner and R. B. Sartor, *The Journal of Immunology*, 1999, **163**, 3474-3483.
11. S. Singh and B. B. Aggarwal, *Journal of Biological Chemistry*, 1995, **270**, 24995-25000.
12. W. B. Song, Y. Y. Wang, F. S. Meng, Q. H. Zhang, J. Y. Zeng, L. P. Xiao, X. P. Yu, D. D. Peng, L. Su, B. Xiao and Z. S. Zhang, *PloS one*, 2010, **5**, e12969.
13. K. Reyes-Gordillo, J. Segovia, M. Shibayama, P. Vergara, M. G. Moreno and P. Muriel, *Biochimica et Biophysica Acta (BBA)-General Subjects*, 2007, **1770**, 989-996.
14. N. Alamdari, P. O'Neal and P.-O. Hasselgren, *Nutrition*, 2009, **25**, 125-129.
15. E. Vazeille, L. Slimani, A. Claustre, H. Magne, R. Labas, D. Bechet, D. Taillandier, D. Dardevet, T. Astruc, D. Attaix and L. Combaret, *The Journal of nutritional biochemistry*, 2012, **23**, 245-251.
16. M. Bayet-Robert and D. Morvan, *PloS one*, 2013, **8**, e57971.
17. B. Jin and Y. P. Li, *Journal of cellular biochemistry*, 2007, **100**, 960-969.
18. Y. Tanaka, H. Eda, T. Tanaka, T. Udagawa, T. Ishikawa, I. Horii, H. Ishitsuka, T. Kataoka and T. Taguchi, *Cancer research*, 1990, **50**, 2290-2295.
19. Y. Quanjun, Y. Genjin, W. Lili, L. Bin, L. Jin, Y. Qi, L. Yan, H. Yonglong, G. Cheng and Z. Junping, *Molecular bioSystems*, 2013, **9**, 3015-3025.
20. Y. Quanjun, W. Lili, Z. Zhiyong, L. Yan, Y. Qi, L. Liya, L. bin and G. Cheng, *Phytomedicine*, 2013, **20**, 992-998.
21. K. Bairwa, J. Grover, M. Kania and S. M. Jachak, *RSC advances*, 2014, **4**, 13946-13978.
22. O. Beckonert, H. C. Keun, T. M. Ebbels, J. Bundy, E. Holmes, J. C. Lindon and J. K. Nicholson, *Nature protocols*, 2007, **2**, 2692-2703.
23. A. M. Weljie, J. Newton, P. Mercier, E. Carlson and C. M. Slupsky, *Analytical chemistry*, 2006, **78**, 4430-4442.
24. N. Psychogios, D. D. Hau, J. Peng, A. C. Guo, R. Mandal, S. Bouatra, I. Sinelnikov, R. Krishnamurthy, R. Eisner, B. Gautam, N. Young, J. Xia, C. Knox, E. Dong, P. Huang, Z. Hollander, T. L. Pedersen, S. R. Smith, F. Bamforth, R. Greiner, B. McManus, J. W. Newman, T. Goodfriend and D. S. Wishart, *PloS one*, 2011, **6**, e16957.
25. M. Meret, D. Kopetzki, T. Degenkolbe, S. Kleessen, Z. Nikoloski, V. Tellstroem, A. Barsch, J. Kopka, M. Antonietti and L. Willmitzer, *RSC advances*, 2014, **4**, 16777-16781.
26. G. Liu, G. Yang, T. Fang, Y. Cai, C. Wu, J. Wang, Z. Huang and X. Chen, *RSC advances*, 2014, **4**, 23749-23758.
27. J. Xia and D. S. Wishart, *Bioinformatics*, 2010, **26**, 2342-2344.
28. T. M. O'Connell, F. Ardeshirpour, S. A. Asher, J. H. Winnike, X. Yin, J. George, D. C. Guttridge, W. He, A. Wysong and M. S. Willis, *Metabolomics*, 2008, **4**, 216-225.
29. C. B. Newgard, J. An, J. R. Bain, M. J. Muehlbauer, R. D. Stevens, L. F. Lien, A. M. Haqq, S. H. Shah, M. Arlotto and C. A. Slentz, *Cell metabolism*, 2009, **9**, 311-326.
30. L. Yi, N. Dong, S. Shi, B. Deng, Y. Yun, Z. Yi and Y. Zhang, *RSC advances*, 2014, **4**, 59094-59101.

RSC Advances Accepted Manuscript

31. Y. Chen, S. Sood, K. McIntire, R. Roth and R. Rabkin, *American journal of physiology. Endocrinology and metabolism*, 2011, **301**, E873-881.
32. H. C. Dreyer, M. J. Drummond, B. Pennings, S. Fujita, E. L. Glynn, D. L. Chinkes, S. Dhanani, E. Volpi and B. B. Rasmussen, *American journal of physiology. Endocrinology and metabolism*, 2008, **294**, E392-400.
33. L. R. Viana and M. C. Gomes-Marcondes, *Biology of reproduction*, 2014.
34. M. S. Kim, K. Y. Wu, V. Auyeung, Q. Chen, P. A. Gruppuso and C. Phornphutkul, *American journal of physiology. Endocrinology and metabolism*, 2009, **296**, E1374-1382.
35. M. Fitzpatrick and S. P. Young, *Swiss medical weekly*, 2013, **143**, w13743.
36. C. Bing, Y. Bao, J. Jenkins, P. Sanders, M. Manieri, S. Cinti, M. J. Tisdale and P. Trayhurn, *Proceedings of the National Academy of Sciences of the United States of America*, 2004, **101**, 2500-2505.
37. L. Laffel, *Diabetes/metabolism research and reviews*, 1999, **15**, 412-426.
38. C. Schaaf, B. Shan, M. Buchfelder, M. Losa, J. Kreutzer, W. Rachinger, G. Stalla, T. Schilling, E. Arzt and M. Perone, *Endocrine-related cancer*, 2009, **16**, 1339-1350.
39. S. M. Wyke and M. J. Tisdale, *British journal of cancer*, 2005, **92**, 711-721.

RSC Advances Accepted Manuscript

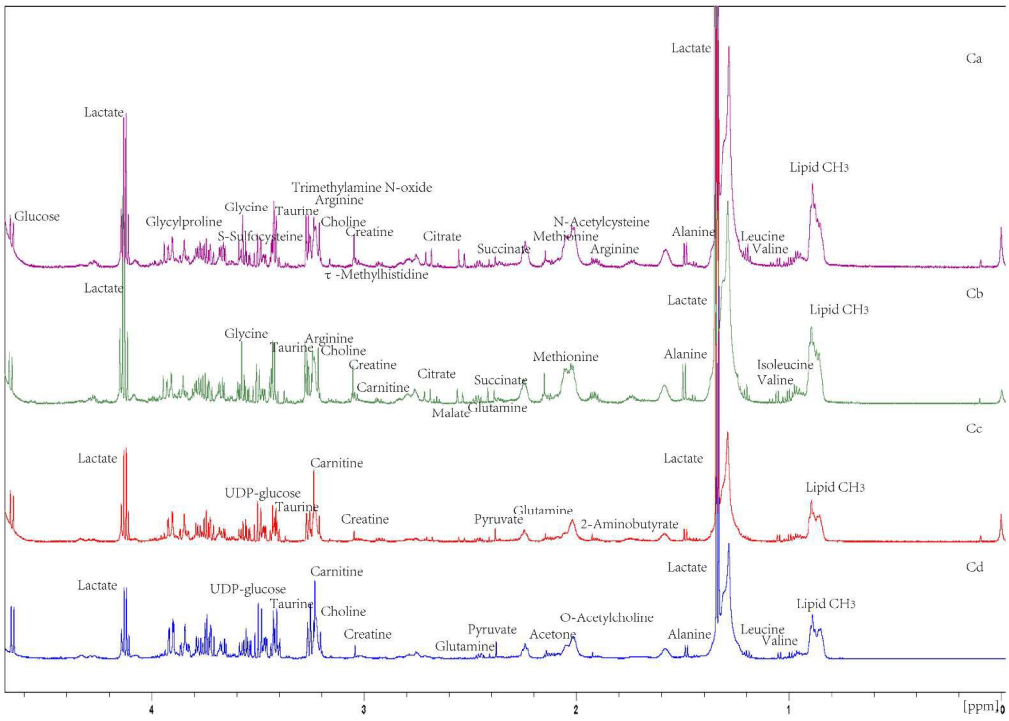

. Representative 600MHz 1H NMR spectrum of serum from cachexia (Ca), curcumin-treated cachexia (Cb) and curcumin-treated control (Cc) and control (Cd) mice. The spectrum displayed a wide range of metabolites such as carbohydrates, lipoproteins, organic acids and amino acids.
294x209mm (300 x 300 DPI)

RSC Advances Accepted Manuscript

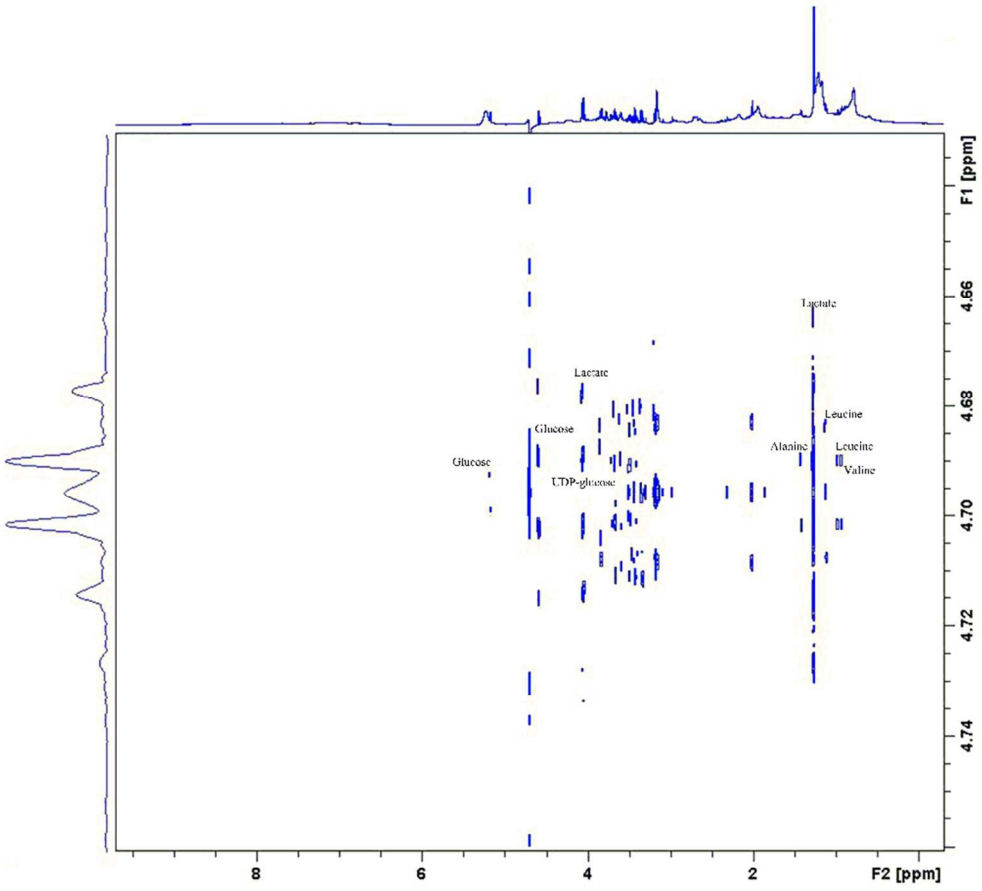

The typical 2D J-resolved NMR spectroscopy of serum metabolites.
86x77mm (300 x 300 DPI)

RSC Advances Accepted Manuscript

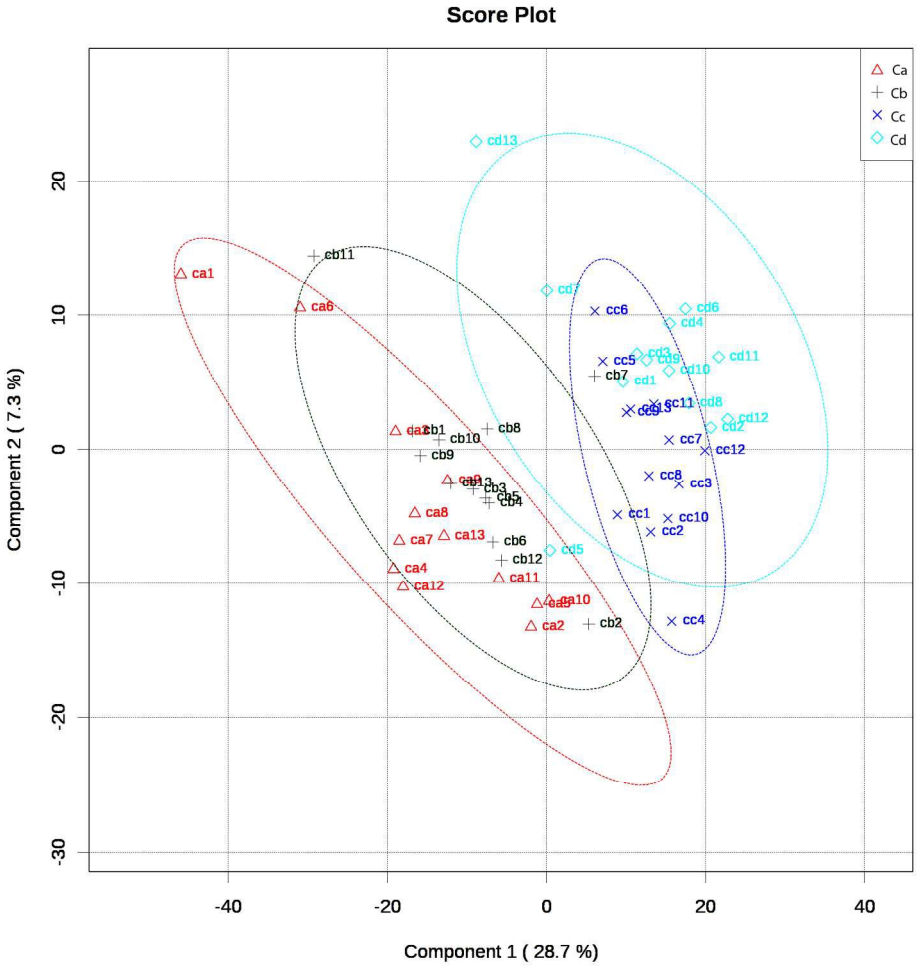

2D PLS-DA score plots showed significant discrimination of the cachexia (Ca), curcumin-treated cachexia (Cb) and curcumin-treated control (Cc) and control (Cd) mice.
740x740mm (72 x 72 DPI)

RSC Advances Accepted Manuscript

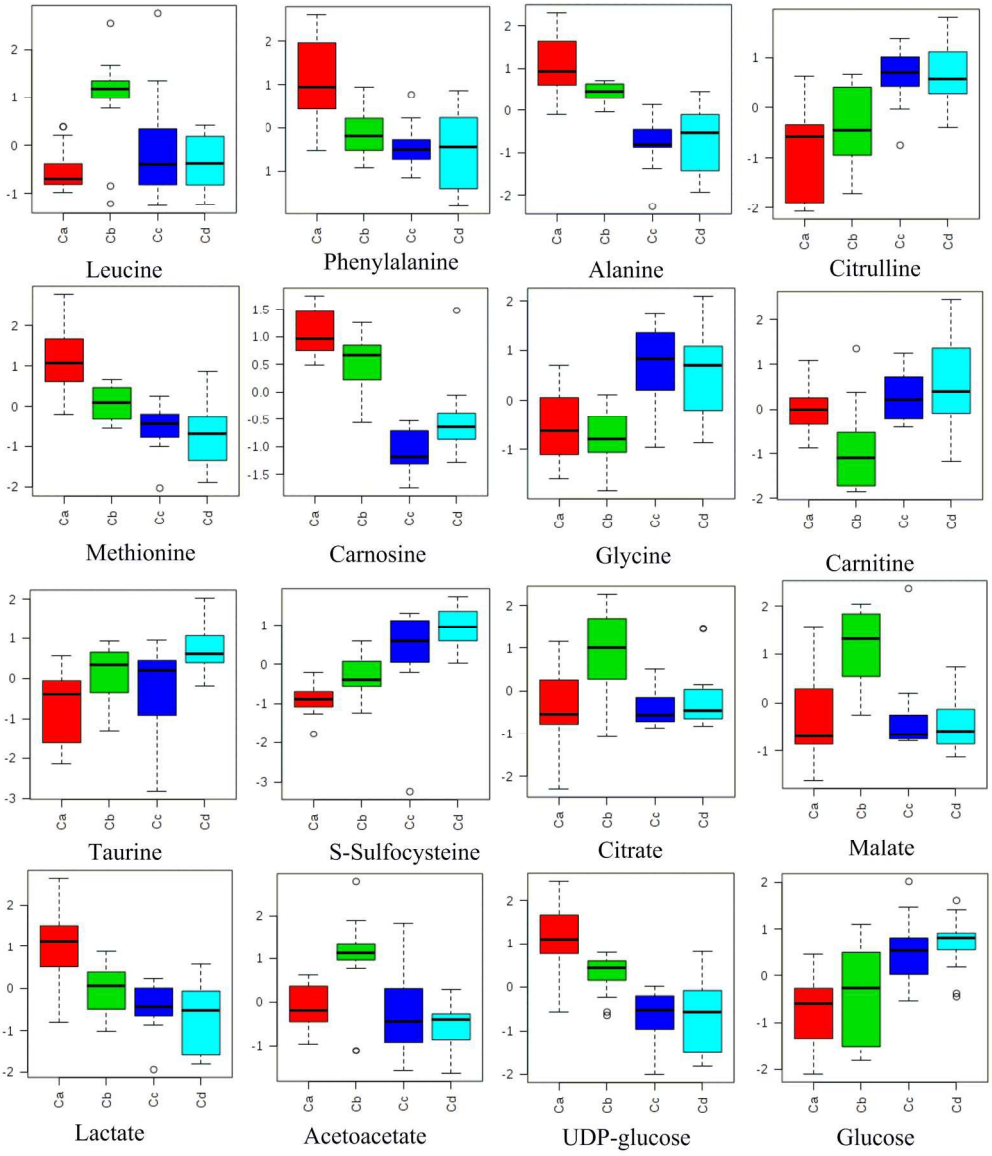

The relative levels of serum metabolites of cachexia (Ca), curcumin-treated cachexia (Cb), curcumin-treated control (Cc) and control (Cd) groups.
177x206mm (300 x 300 DPI)

RSC Advances Accepted Manuscript

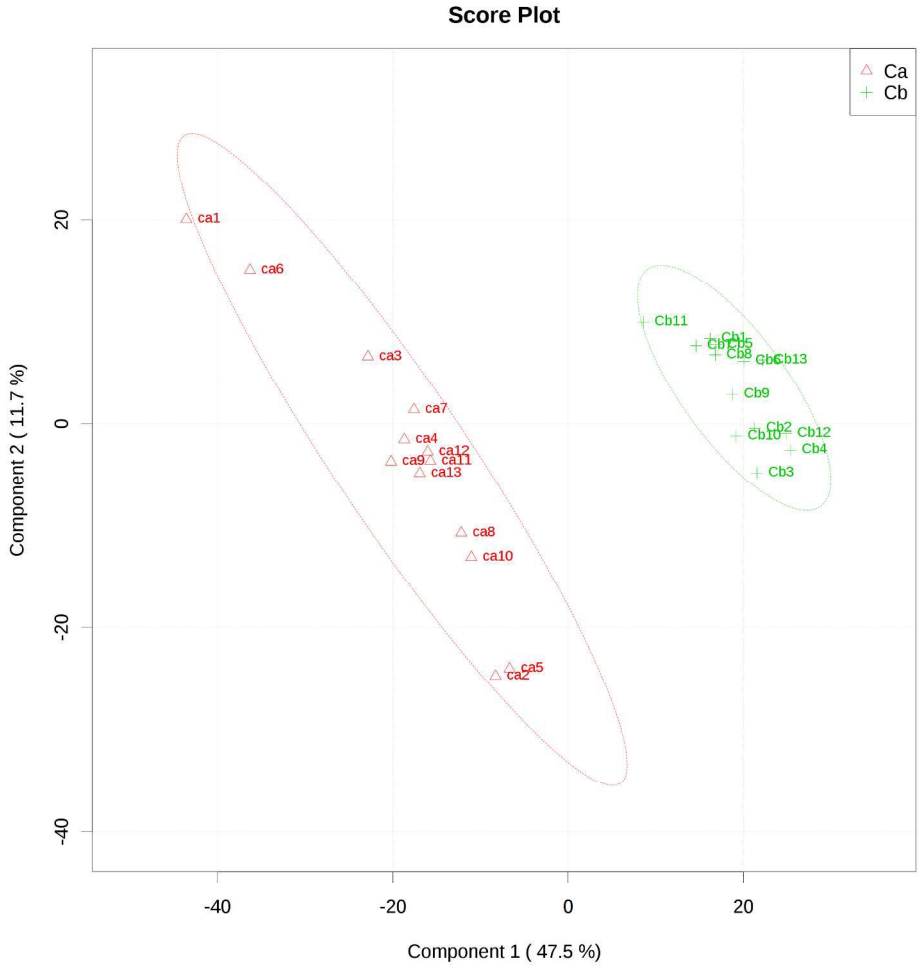

The PLS-DA score plots between two groups: cachexia (Ca) and curcumin-treated cachexia (Cb) revealed the curcumin effect on cancer cachexia mice (A),
952x952mm (72 x 72 DPI)

RSC Advances Accepted Manuscript

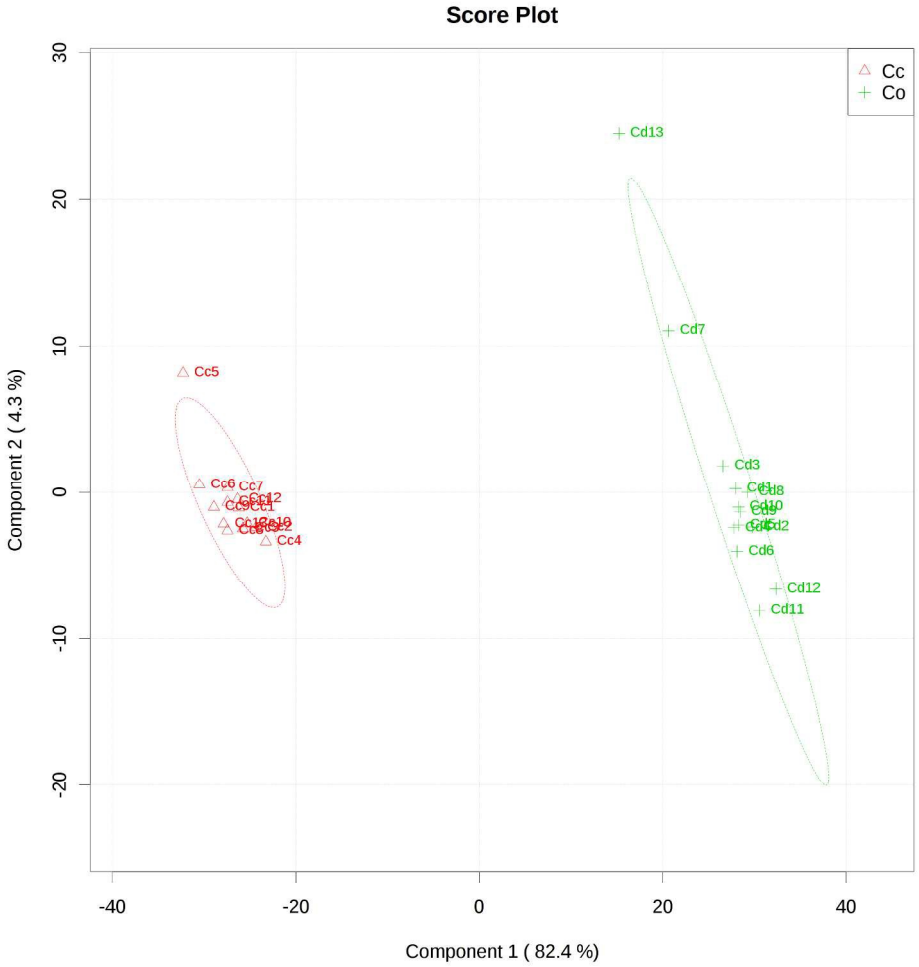

The PLS-DA score plots between two groups: control (Cd) identified regulation of curcumin on control mice.
952x952mm (72 x 72 DPI)

RSC Advances Accepted Manuscript

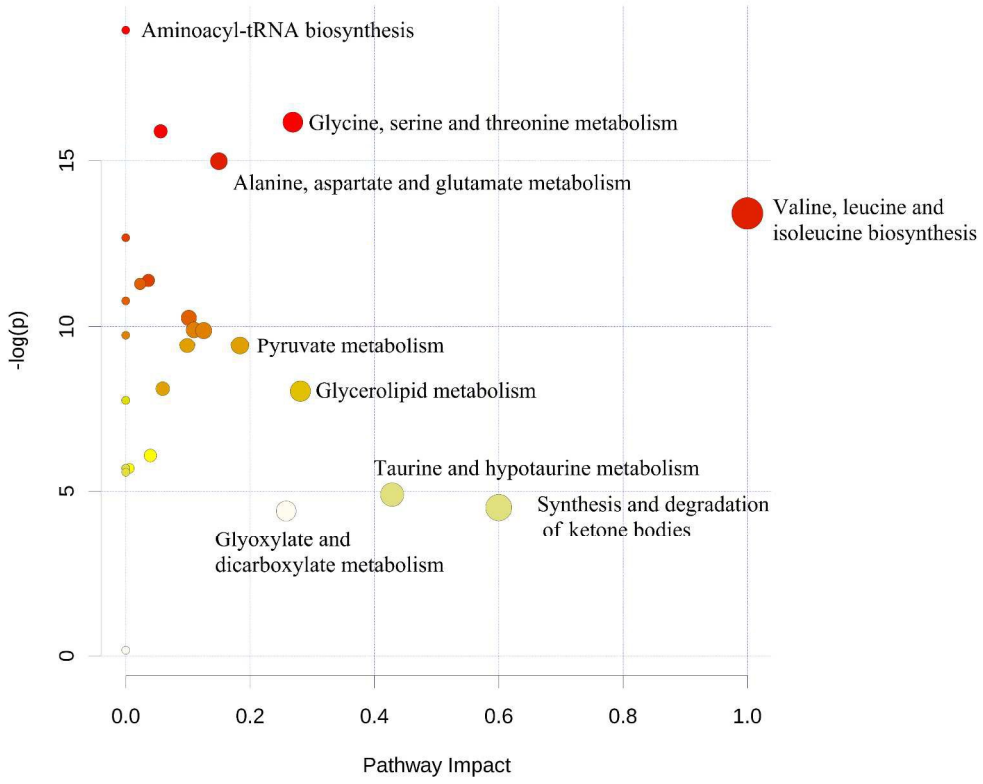

The perturbed metabolic pathways of cachexia and the effect of curcumin. The X axis was the impact factor and the Y axis was the –log(p).
254x220mm (300 x 300 DPI)

RSC Advances Accepted Manuscript

NMR-Based Metabolomics Reveals Distinct Pathways Mediated by Curcumin in Cachexia Mice Bearing CT26 Tumor

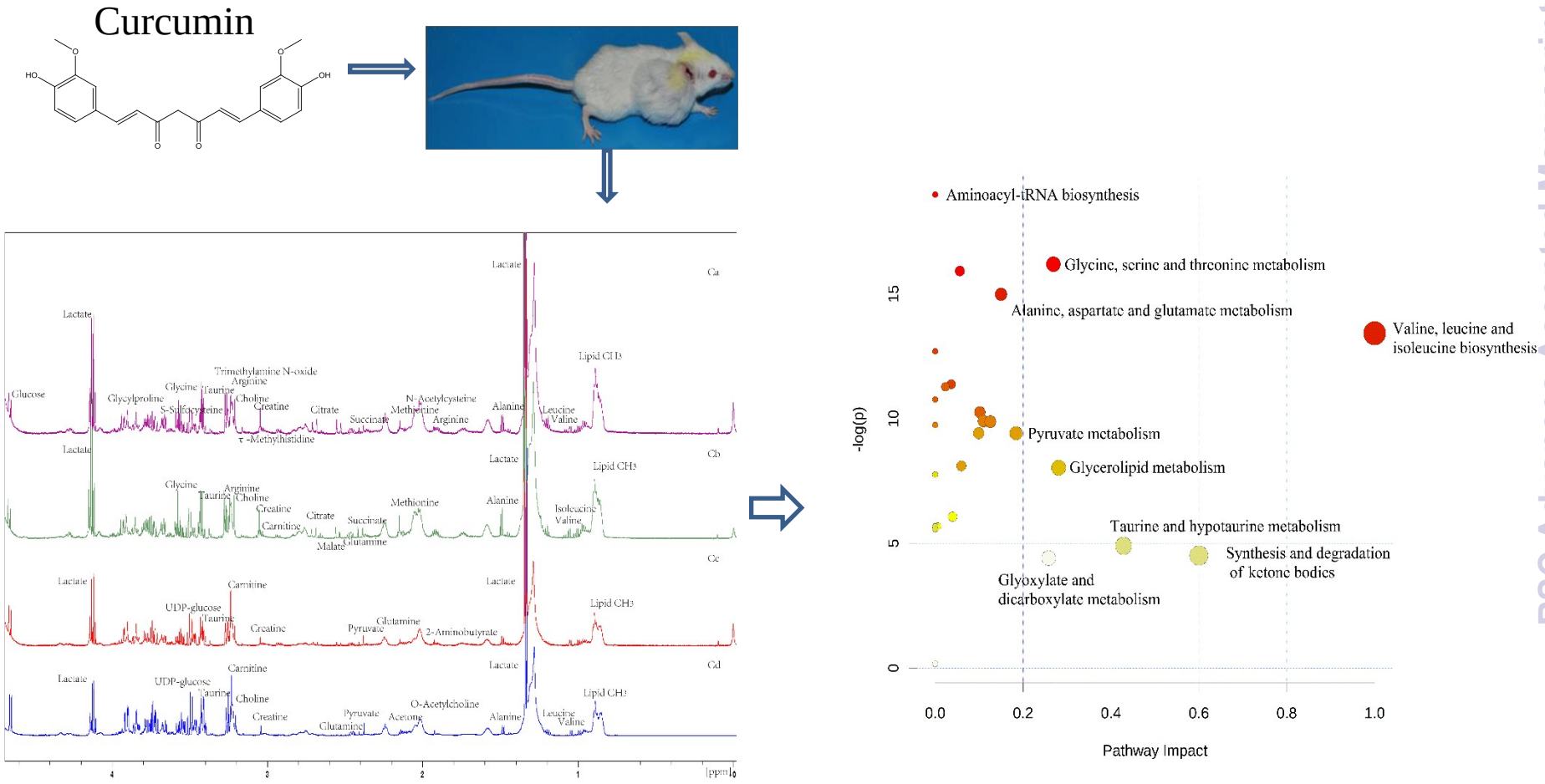

Graphical Abstract

RSC Advances Accepted Manuscript